THERMAL AND FLUID MODELING OF THE CRYogenic Orbital TEstbed (CRYOTE) GROUND TEST ARTICLE (GTA)

David Piryk, a.i. Solutions (KSC)
Paul Schallhorn, Launch Services Program (KSC)
Laurie Walls, Launch Services Program (KSC)
Benny Stopnitzky, United Launch Alliance
Noah Rhys, Yetispace Inc. (MSFC)
Mark Wollen, Innovative Engineering Solutions

Executive Summary

The purpose of this study was to anchor thermal and fluid system models to data acquired from a ground test article (GTA) for the CRYogenic Orbital TEstbed – CRYOTE. To accomplish this analysis, it was broken into four primary tasks. These included model development, pre-test predictions, testing support at Marshall Space Flight Center (MSFC) and post-test correlations. Information from MSFC facilitated the task of refining and correlating the initial models.

The primary goal of the modeling/testing/correlating efforts was to characterize heat loads throughout the ground test article. Significant factors impacting the heat loads included radiative environments, multi-layer insulation (MLI) performance, tank fill levels, tank pressures, and even contact conductance coefficients. This paper demonstrates how analytical thermal/fluid networks were established, and it includes supporting rationale for specific thermal responses seen during testing.

Introduction and Background Information

CRYOTE Flight Article Overview

ULA, in partnership with several NASA centers and industry, proposed the Cryogenic Orbital Testbed project specifically to develop cryogenic fluid management (CFM) technologies. CRYOTE would serve as a demonstration platform for critical CFM technologies such as system chilldown, transfer, health management, pressure control, active cooling and long term storage. To keep launch costs down, CRYOTE would share unused room with a primary satellite – inside the fairing of an upper stage rocket, such as the Centaur. Figure 1 below shows an Atlas V and CRYOTE launch configuration. After primary payload separation, residual liquid hydrogen from the Centaur is transferred to CRYOTE's tank (Reference 1).

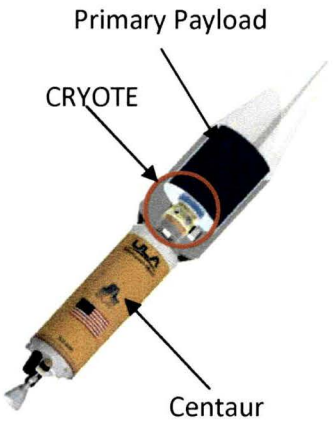

Figure 1: Proposed CRYOTE Launch Configuration – Atlas V EELV

CRYOTE Ground Test Article Overview

Innovative Engineering Solutions (IES) and NASA KSC jointly developed and built the CRYOTE ground test article, shown below, in Figure 2. The mockup consisted of a titanium alloy tank, composite skirt (similar to G10), an external secondary payload adapter (ESPA) ring, thermal vent system (TVS), MLI and a range of data acquisition instruments. To understand heat loads throughout the system, the GTA was filled with liquid nitrogen (for safety purposes) and then tested in a vacuum chamber at Marshall Space Flight Center. Higher fidelity predictions about the thermal environment of future flight articles could be made by anchoring analytical models against test data.

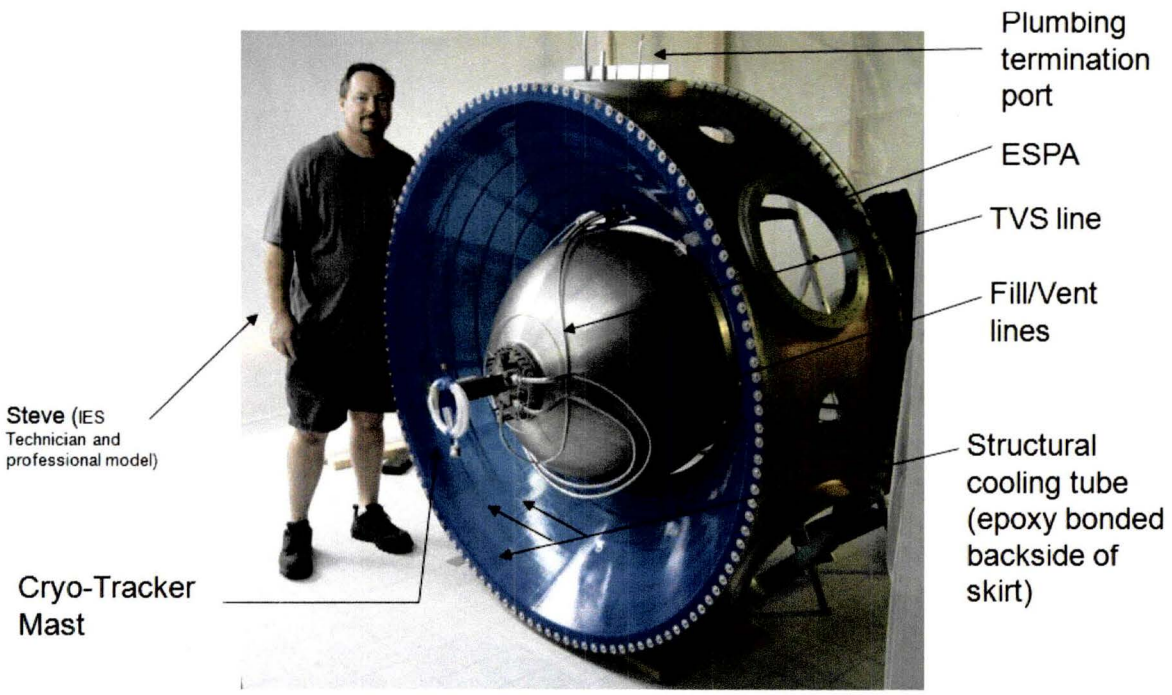

Figure 2: CRYOTE Ground Test Article and Instrumentation (excluding MLI)

To prevent cryogenic fluids from boiling off, proper heat rejection systems were included on the test article. NASA KSC's Cryogenic Laboratory and Innovative Engineering Solutions designed and built proper heat rejection systems to prevent cryogenic reserves from boiling off.

Primary protection came in the form of MLI blankets. Four sub-blankets and an outer Beta cover enclosed the tank and composite skirt. Each sub-blanket consisted of five double aluminized Mylar layers separated by double Dacron netting (Reference 2). In addition to MLI blankets, a thermal vent system (TVS) was also installed to actively cool skirt structures with boil-off gas.

Testing was conducted at Marshall Space Flight Center because the Exploration Systems Test Facility (ESTF) had a large enough vacuum chamber to house the GTA. In addition, this facility demonstrated it could achieve necessary vacuum levels (less than $1x10^{-5}$torr) to simulate pressures at orbital altitude. These environments were especially important for optimum MLI performance. Figure 3 shows a general layout of the ESTF. Figure 4 shows CRYOTE GTA installed in the vacuum chamber (Reference 3).

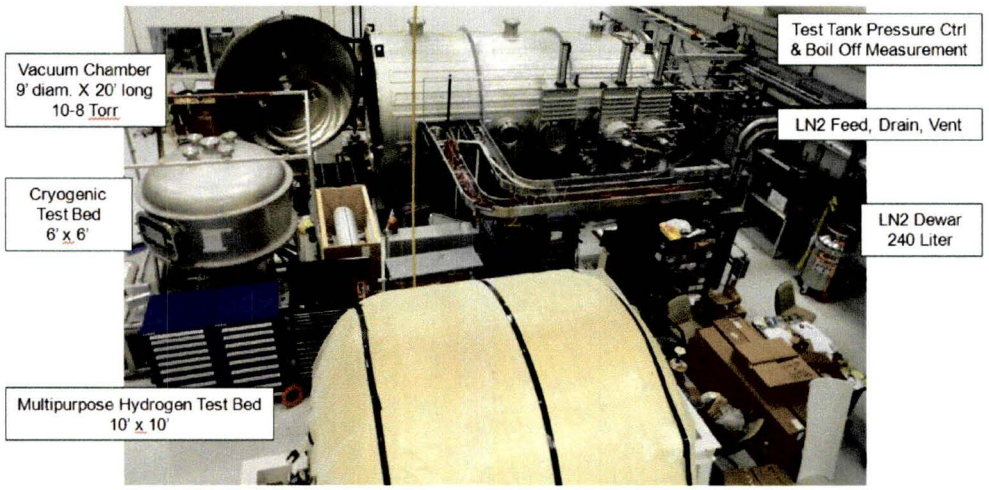

Figure 3: Marshall Space Flight Center's Exploration Systems Test Facility

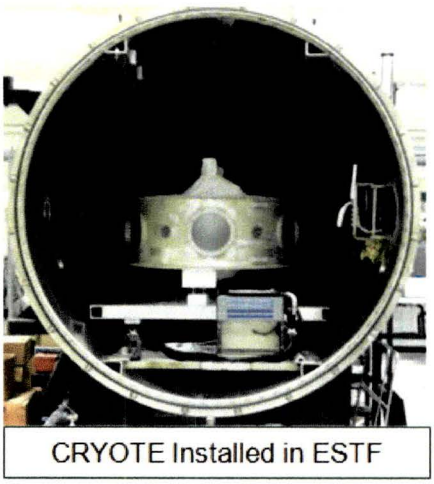

Figure 4: CRYOTE GTA Installed in ESTF Vacuum Chamber

Thermal/Fluid Math Models

Following MSFC testing, preliminary modeling work showed strong correlation between predicted heat loads and actual heat loads to LN_2 in CRYOTE GTA. Predicted steady state heat loads indicated 98% agreement with actual test data. Despite excellent correlation for total heating rates to liquid nitrogen (LN_2) in the tank, additional fidelity had to be added to correlate location-specific thermocouple data.

First, thermal gradients along skirt surfaces were of particular interest. On the test article, five thermocouples spanned the length of the skirt conical section. This line of thermocouples was placed between mounting tabs which would theoretically capture warmest temperatures on the skirt. To correlate a model to these specific locations, the skirt was broken into 32 angular sections and nearly 50 longitudinal sections. This translated to approximately 2.5-3.0 in^2 per TD node along the skirt. Figure 5, below, shows a refined thermal mesh.

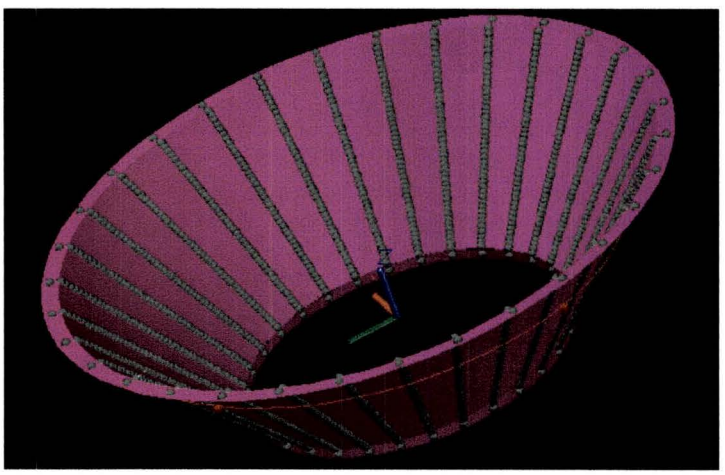

Figure 5: Post-Test Skirt Mesh Quality

In addition to a refined thermal mesh on the skirt, fill and vent lines were added to account for transients (in pressure, temperature, and liquid reserve quantities) during filling operations. Fill and vent lines were attached to the skirt surfaces at four distinct locations. Mounting locations in analytical models appropriately correspond to physical mounting locations on the GTA hardware. Figure 6 below illustrates this addition. During fill operations, one line was appropriately held at LN_2 temperatures.

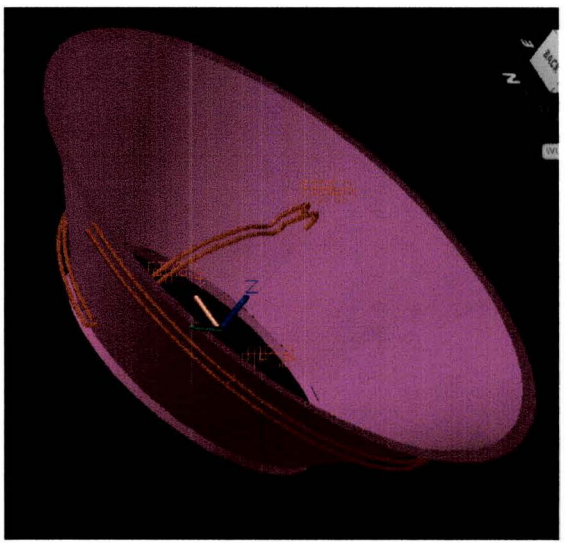

Figure 6: CRYOTE GTA Fill and Vent Lines

Next, design drawings were readily available for each of the four MLI sub-blankets. In efforts to accurately model exposed surface areas (to radiative environments, and blanket to tank), each blanket was assigned unique Thermal Desktop surfaces. Based on a modified Martin equation, each blanket had an effective emissivity value associated with it. Table 1 below characterizes surface finishes between blankets.

Blanket	Inner Finish	Outer Finish
1 - Innermost	Aluminized MLI	Aluminized MLI
2	Aluminized MLI	Aluminized MLI
3	Aluminized MLI	Aluminized MLI
4 - Outermost	Aluminized MLI	Beta Cloth

Table 1: MLI Blanket Characteristics

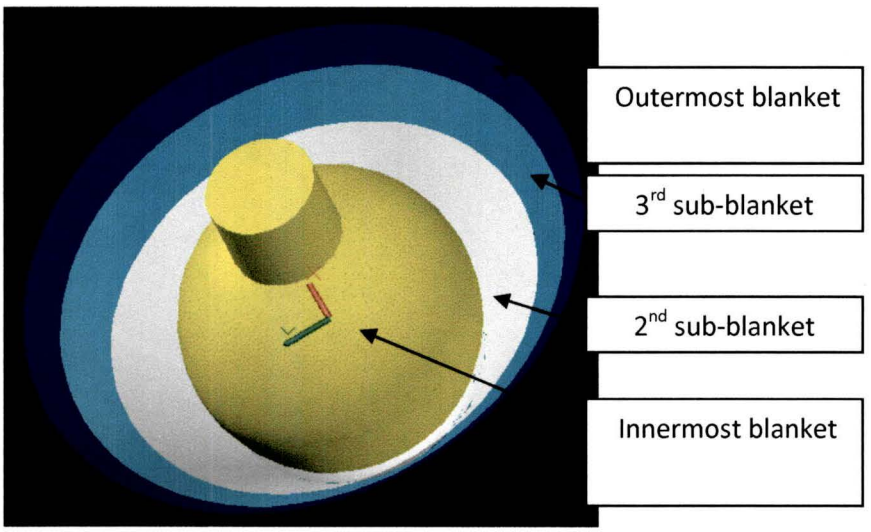

Figure 7: MLI Sub-Blankets (Bottom)

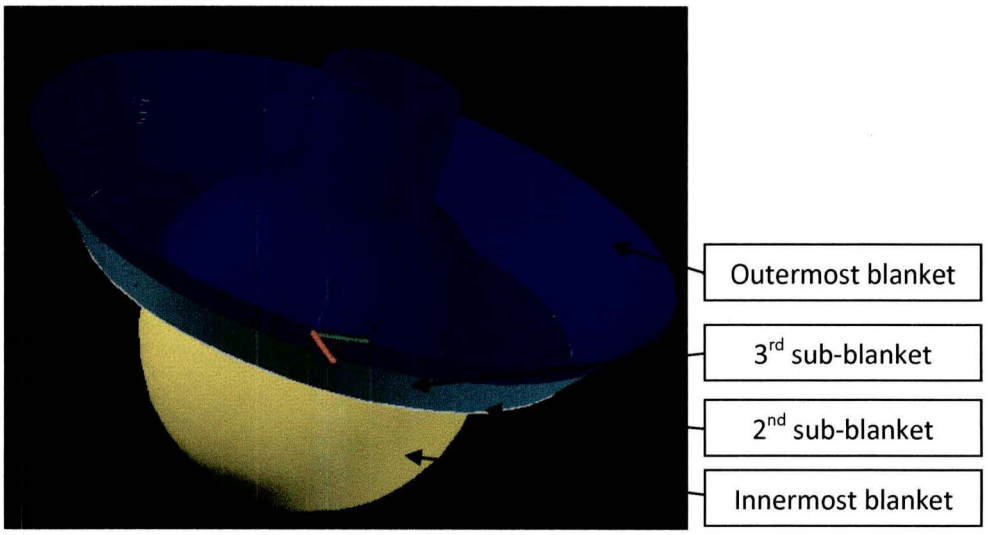

Figure 8: MLI Sub-Blankets (Top)

After MLI surfaces were added, tank modeling was the last major effort. Since a higher fidelity thermal model was in place, it was only fitting that a higher fidelity fluid model be developed as well. For post-test efforts, TD tank surfaces were broken down into 20 equal surface areas (longitudinally). In addition, a 'fill' variation of the model added a fluid lump/sub-tank with each segment. To reduce run times for steady state modeling, a two lump approach was used (bulk liquid/vapor) to characterize nitrogen phases. Figures 9 and 10 illustrate final tank models.

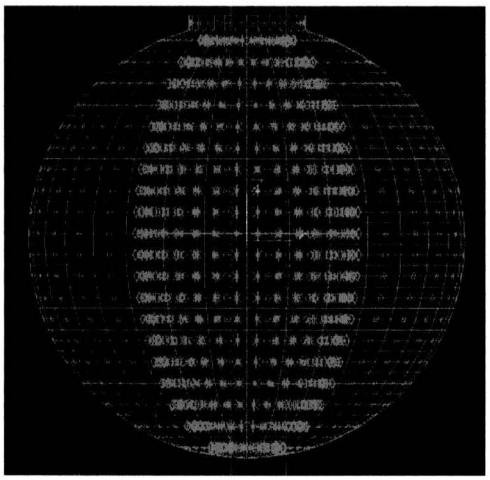

Figure 9: Tank Fill Model – 20 Lumps

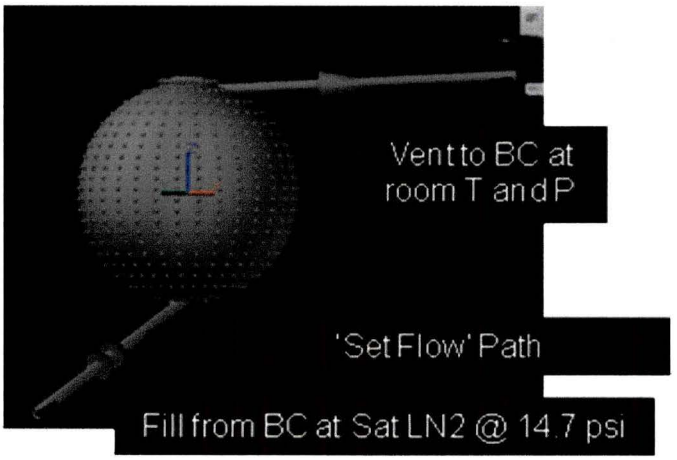

Figure 10: Tank Fill Model Showing Set Flow and Vent/Fill BC's

CRYOTE GTA Results Summary and Conclusions

Model Specific Correlation Parameters

Specific parameters in Thermal Desktop needed to be adjusted to satisfy steady state model-to-test data correlation. Two of the specific parameters included the effective emissivity value associated with MLI blankets and the contact conductance value associated with skirt-to-tank interfaces. In general, these were the two main parameters that needed to be 'dialed in'. Other influencing factors included vacuum chamber temperature, tank pressure and thermophysical/optical properties. For purposes of this analysis, these parameters were considered bounding conditions in accordance to actual test conditions.

Skirt-to-tank contact conductance coefficients were important because they were the primary interface from a relatively hot skirt surface to a relatively cold tank surface. To correlate contact conductance values associated with skirt-to-tank interfaces, test data from thermocouple (TC) 07 were used as reference data points. First, linear conductance values associated with skirt and tank flange surfaces were calculated by applying Fourier's Law (on conduction heat transfer). After that, conductive heat transfer coefficients between the two interfaces were altered until steady-state modeling data corresponding to TC07's location matched test data. After observing a close enough correlation between modeling data and test data, a final contact heat transfer coefficient was found. The contact coefficient found was deemed reasonable considering skirt surfaces were machined and in relatively good contact with tank flange areas (fastened by two nuts and bolts on each flange and torqued to specification).

Finally, effective emissivity (e*) values associated with MLI blankets were first calculated by Martin's equations for e*. This formula calculated e* values based on surface finishes of MLI blankets and the number of layers in each blanket (also ΔT between top/bottom surfaces). Effective emissivity

values associated with each blanket were correlated by heat rate-to-LN_2 test data. Since the outer blanket had a final Beta cover, it did not possess the same e* value as the inner three blankets. As a result, e* values associated with each blanket were proportionally adjusted until modeling data showed positive correlation to test data at steady state.

Test Data vs. Correlated Models

Two primary models were used in post-test correlation efforts. The first was a fill model, which was necessary to estimate initial transients throughout the GTA. Since temperatures along skirt surfaces were of interest, understanding fill line impacts near local attach points was necessary. Intuitively, tank surfaces in contact with LN_2 would reach LN_2 temperature relatively quickly (within a couple seconds) since tank side-wall thicknesses were on the order of 0.1" thick. Figure 11 graphically illustrates the modeled fill rate data against test data. This plot represents LN_2 mass present in the tank relative to time. As seen from test data, there was a small amount of LN_2 in the tank before a fill operation was conducted. This was due to the test team at MSFC having to replace a flow meter prior to testing. As a result, LN_2 was present in fill lines and was slightly cooling down skirt surfaces prior to a proper fill attempt. Despite this, skirt surfaces were only a few degrees cooler over that interval, and did not present significant differences in the times they took to reach steady state temperatures. For modeling purposes, filling operations were assumed to start at about 0.3 hours into any transient analytical run.

Figures 12-15 graphically illustrate temperatures along skirt surfaces. Thermocouple 07 on the test article was located on the outer surface of the bottommost ring where tank and skirt surfaces meet. Thermocouple 11 was located on the uppermost skirt surface, where skirt and ESPA ring interfaces were situated. Between these two thermocouples were TCs 8-10. As observed, temperatures determined analytically correlated very well to final, steady state temperatures. In each figure, a noticeable trend indicated that test temperatures reached steady state sooner than analytical models.

The material properties of the skirt surfaces were the primary reason for this outcome. Since the information was not readily available for the LOX compatible composite used, a G-10 temperature-dependent data set was used. From comparisons made in Figures 11-14, it was reasonable to assume the actual material had a lower heat capacity than G-10. Figure 20 contains information on the parametric analysis conducted for skirt material properties. Another noteworthy observation on test data from Figure 14 (TC09) was a change in temperature response at about four hours. This response change was due to residual LN_2 in the fill line (after fill operations were complete). Once LN_2 in the line flashed off, temperature responses were nominal until steady state was achieved. The supporting data behind this disturbance came from the understanding that TC09 was within 1-2" from a fill/vent line mounting location (Figure 16). Responses observed in TC09 were more pronounced since the sensor was closer to colder fill/vent lines as compared to other thermocouples.

To verify incident heating rates on tank walls, and the LN_2 enclosed within, the MSFC test team used two methods. The first was measuring flow rates of nitrogen gas emanating from a specified vent line location. Here, local temperatures and pressures were known. These parameters were important

[to check gaseous nitrogen (GN_2) density)]. Figure 17 illustrates actual and correlated boil-off rates of LN_2.

The second method was measuring the LN_2 tank mass. Load cells were used to record LN_2 mass changes. Figure 18 illustrates test data from these measurements along with analytical results using a predetermined initial tank mass. As seen, test data and analytical results shared nearly identical responses with regards to tank mass vs. time.

Finally, an analytical trade study was conducted to estimate steady state heating rates to LN_2 at various fill levels. At an 80% fill level by volume, nearly 45% of heat leak to tank surfaces came from skirt-to-tank interfaces. Figure 19 graphically illustrates steady state heating rates with respect to percent full levels (by volume). To minimize heat leak in future tests, a thermally non-conductive material should be placed in between skirt and tank flange interfaces.

References

1.) CRYOTE Concept. Bernard Kutter, Mark Wollen, Noah Rhys and Laurie Walls. 2009.
2.) CRYOTE MLI Design Review. Wes Johnson. NASA KSC Cryogenics Test Laboratory. 2010.
3.) CRYOTE Midterm Review. Noah Rhys. 2011

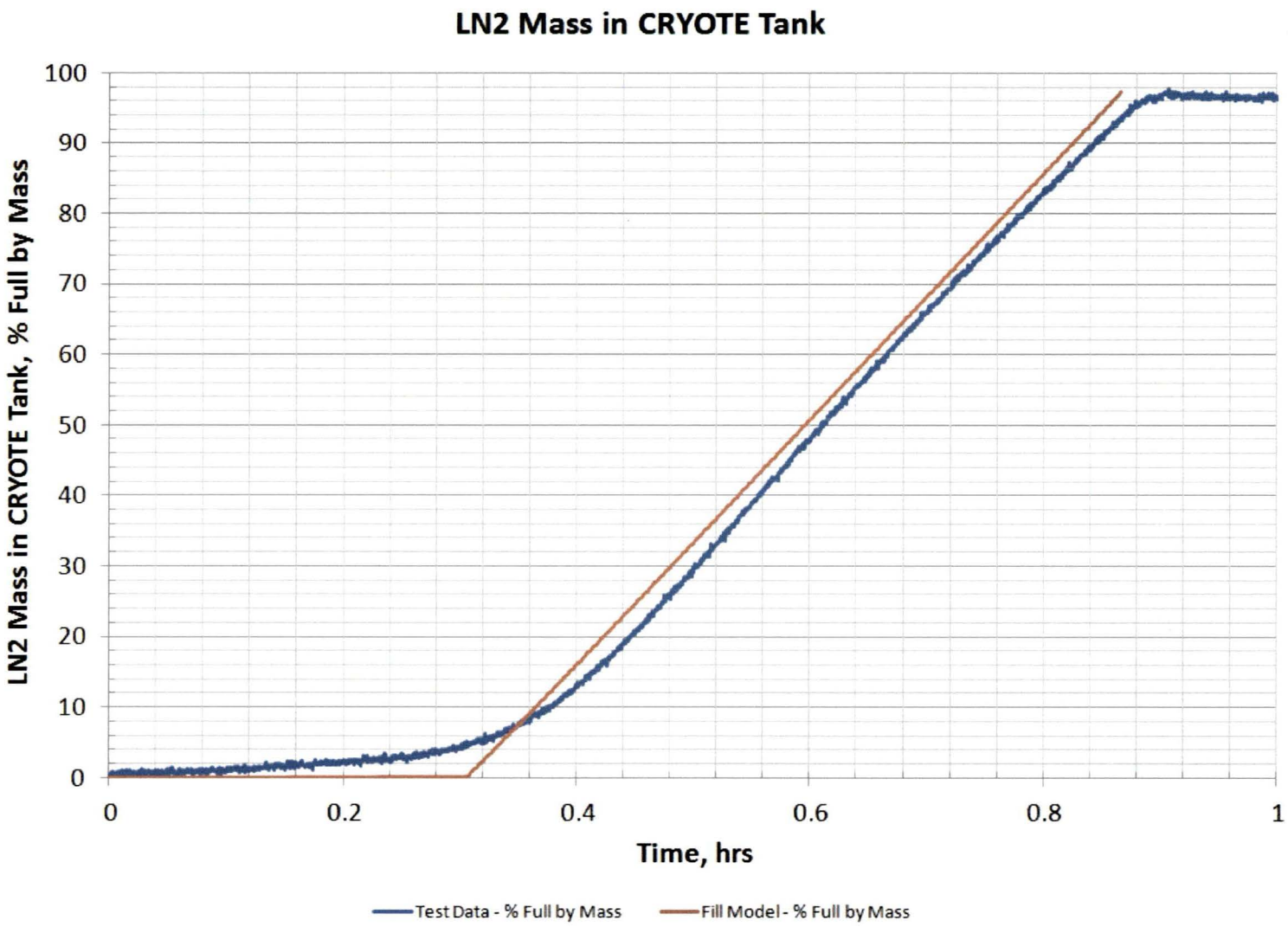

Figure 11: LN2 Mass During Fill Operations – Test vs. Model Correlation

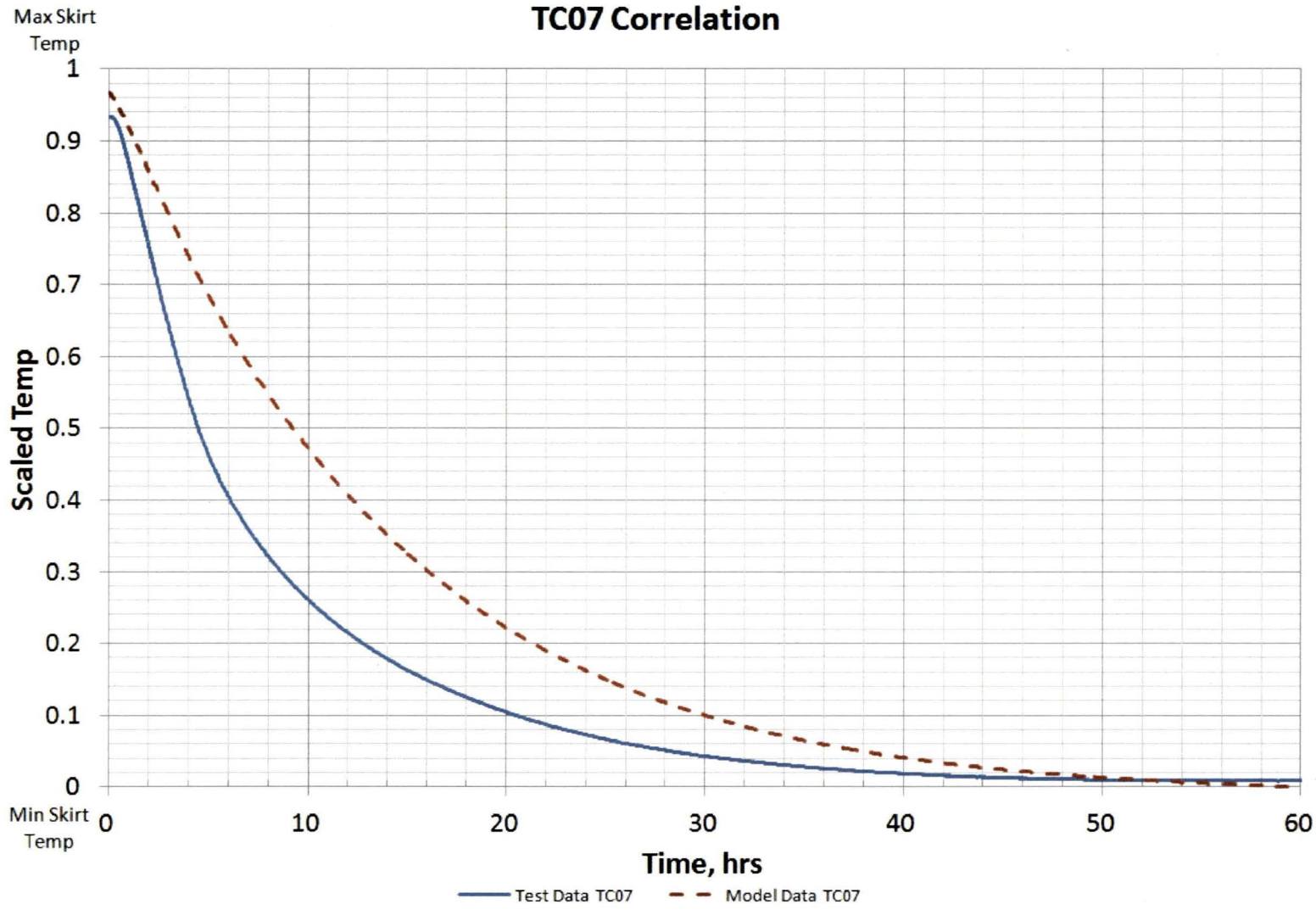

Note: Min/max skirt temps correspond to min/max temps seen from TC07-TC11

Figure 12: TC07 Temperature – Test vs. Analytical Model Correlation

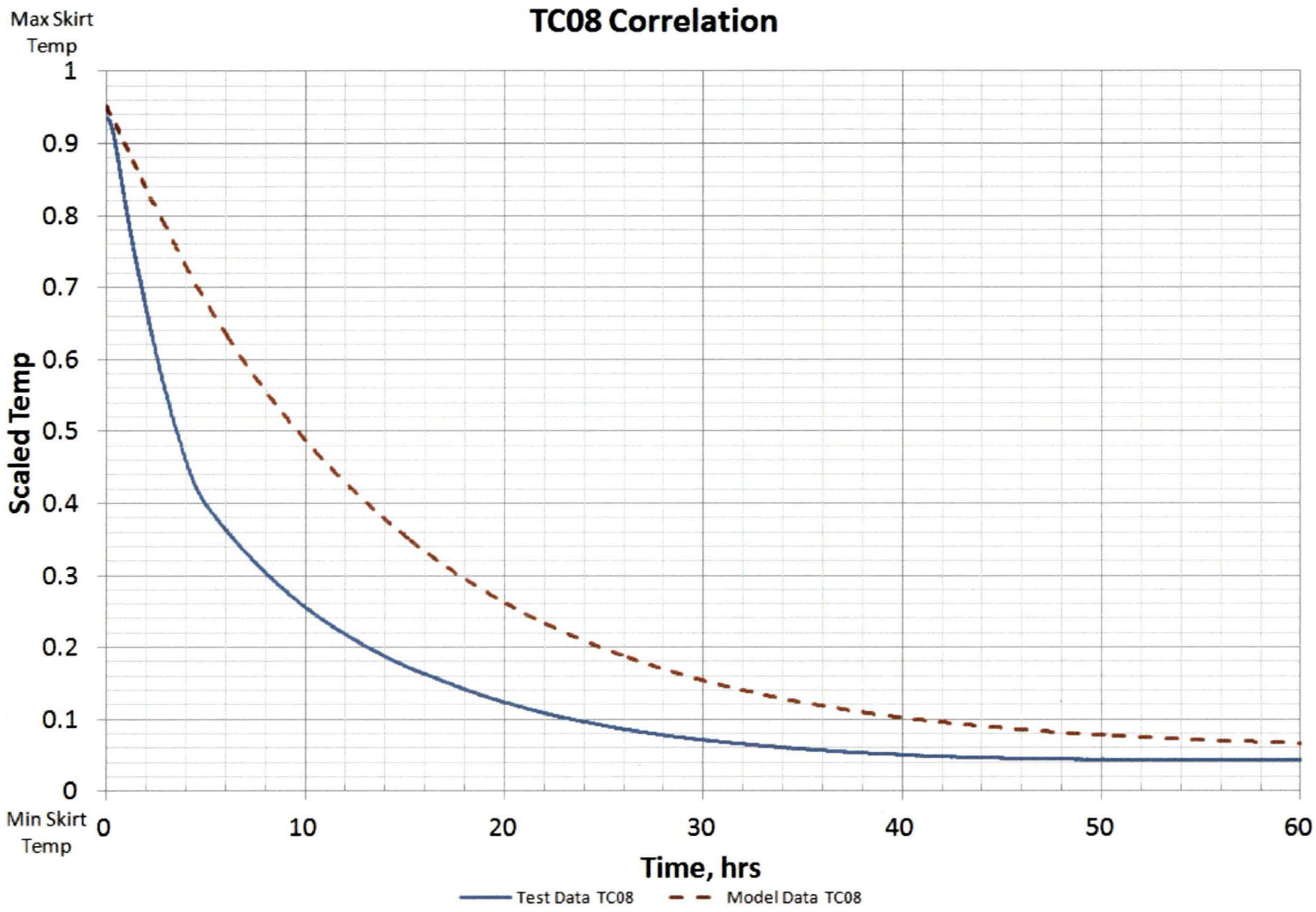

Note: Min/max skirt temps correspond to min/max temps seen from TC07-TC11

Figure 13: TC08 Temperature – Test vs. Analytical Model Correlation

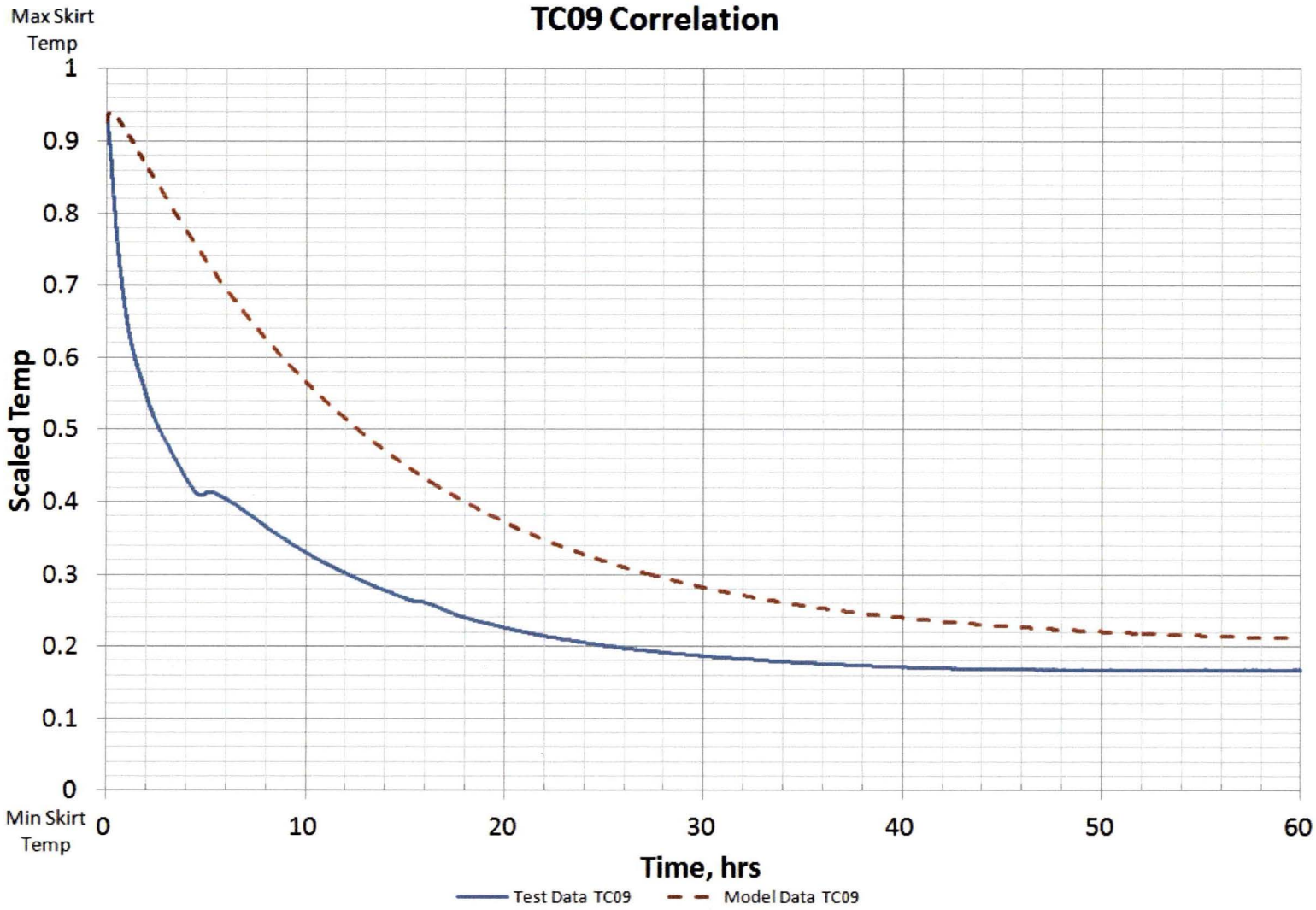

Note: Min/max skirt temps correspond to min/max temps seen from TC07-TC11

Figure 14: TC09 Temperature – Test vs. Analytical Model Correlation

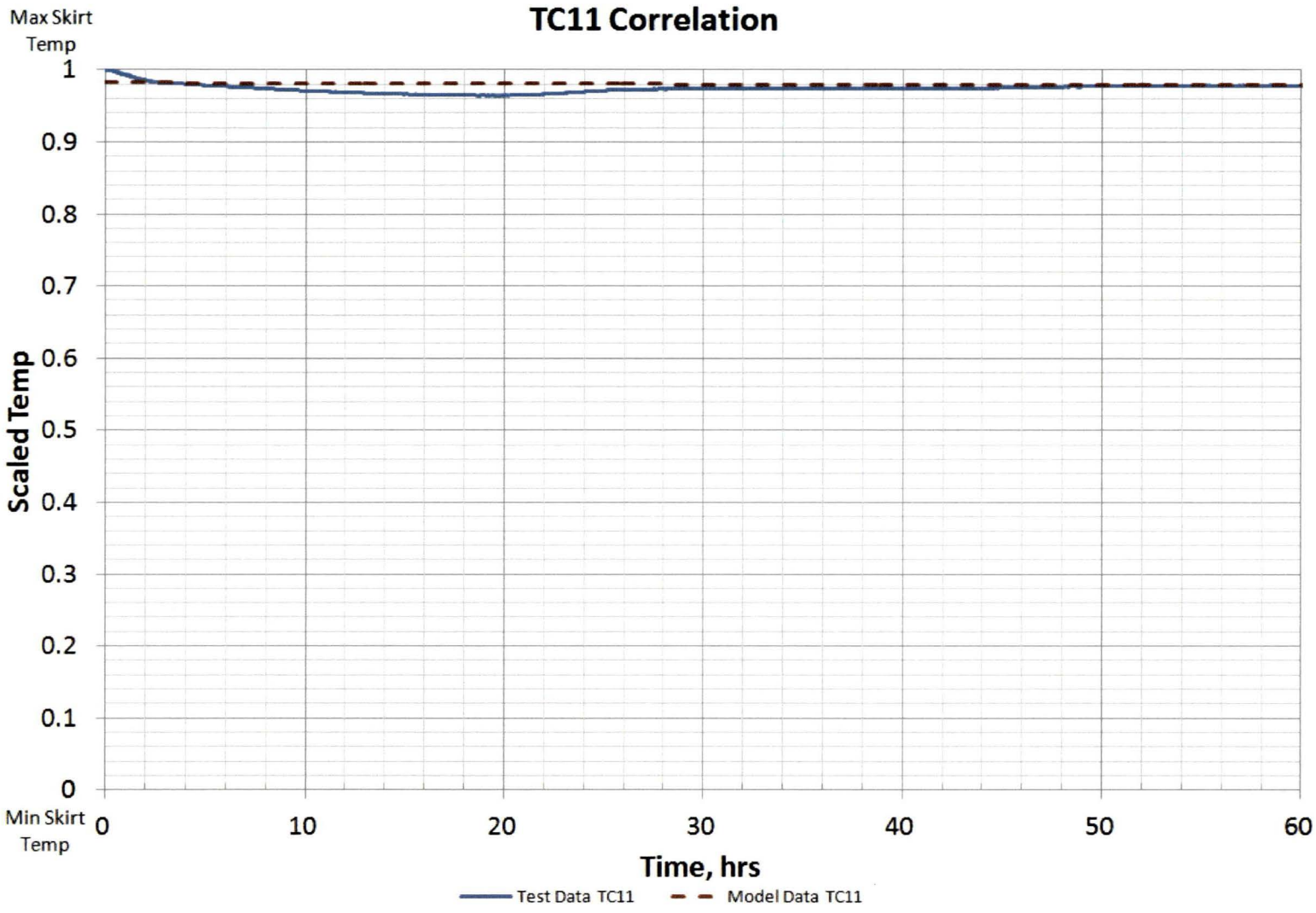

Note: Min/max skirt temps correspond to min/max temps seen from TC07-TC11

Figure 15: TC11 Temperature – Test vs. Analytical Model Correlation

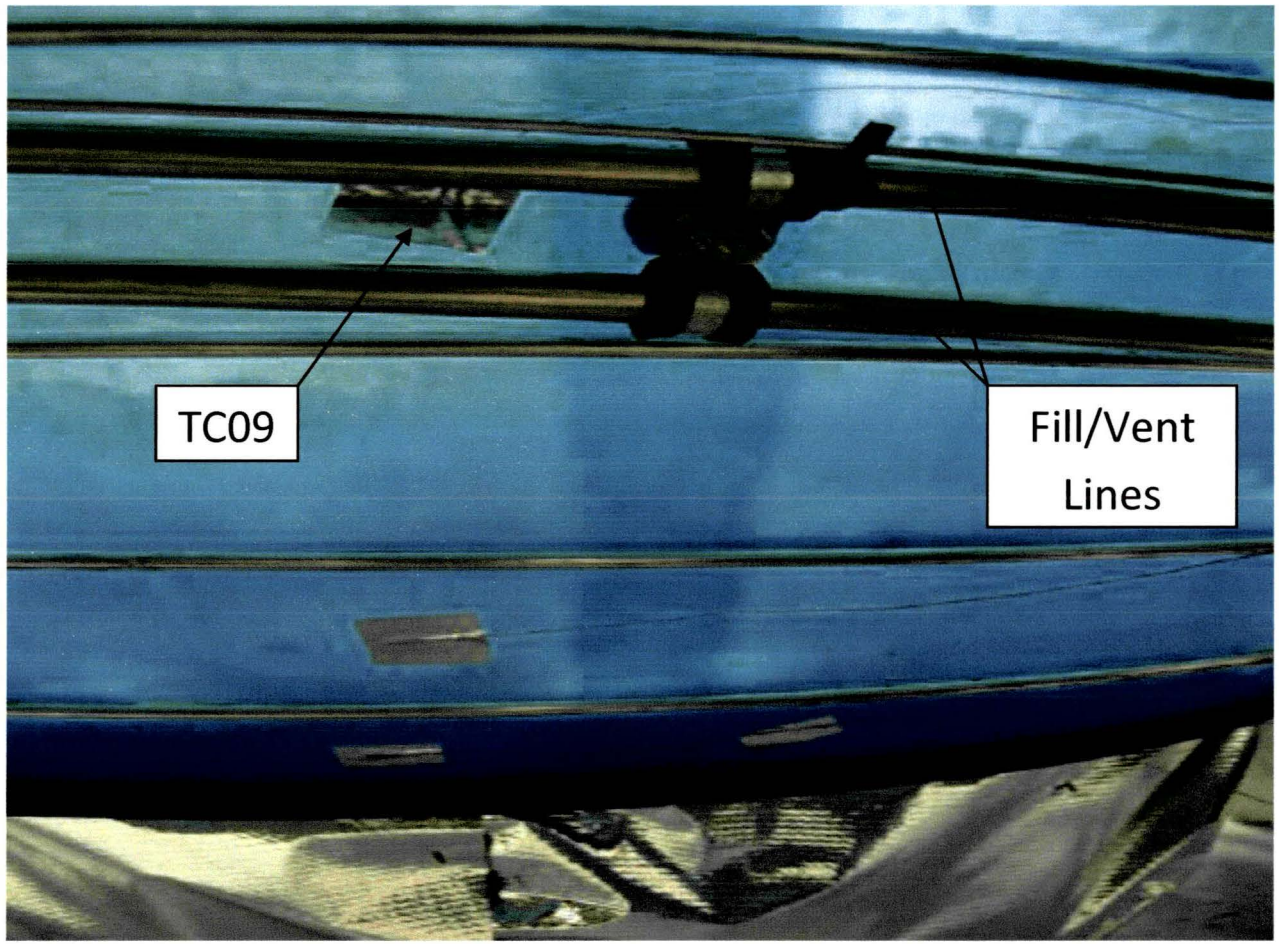

Figure 16: TC09 Location With Respect to Fill/Vent Lines

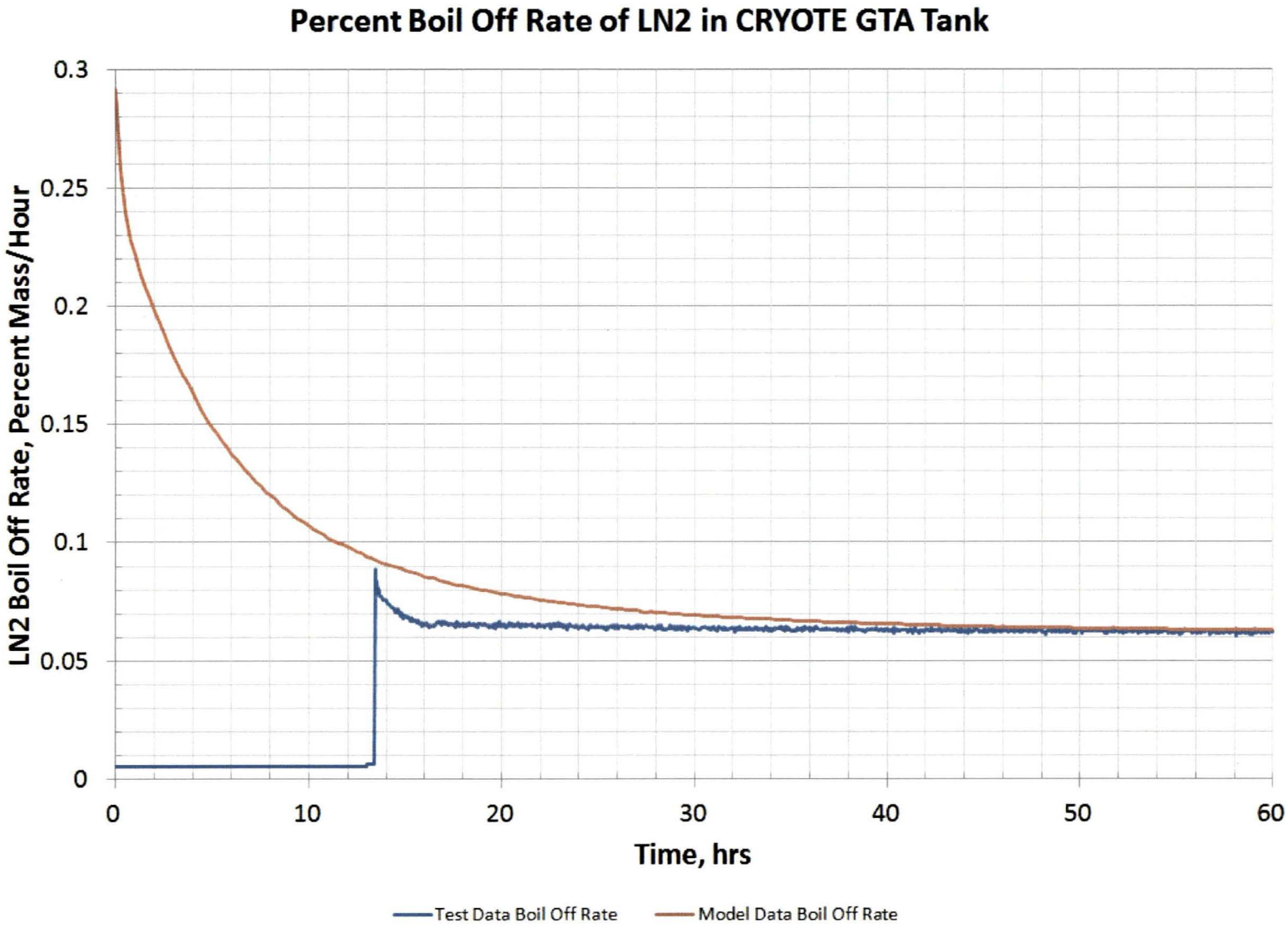

Figure 17: Heat Leak to LN2 – Translated Vent Flow Test Data vs. Analytical Model Boil Off Correlation

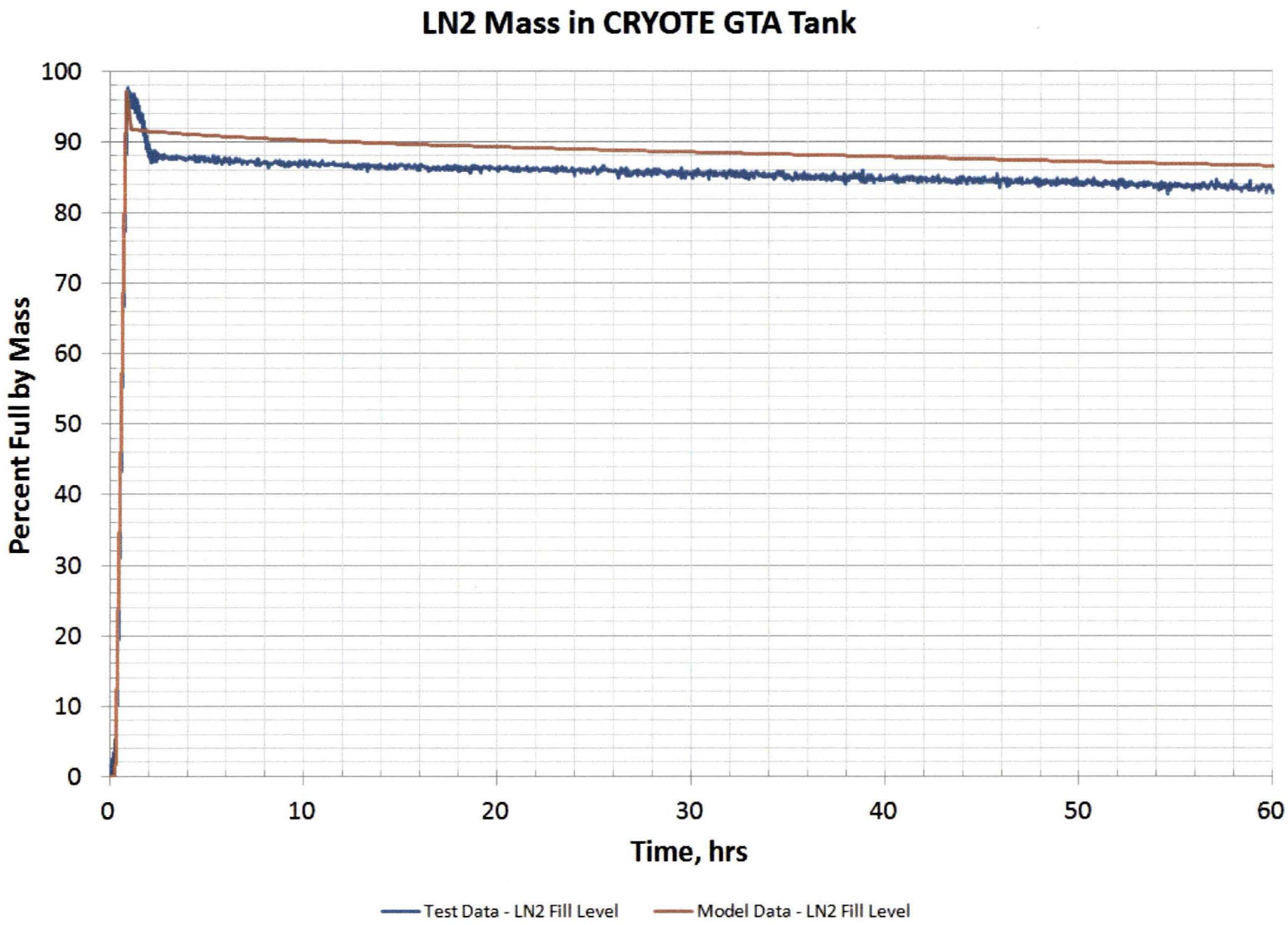

Figure 18: Total LN2 Mass in Tank – Load Cell Test Data vs. Analytical Model Mass Correlation

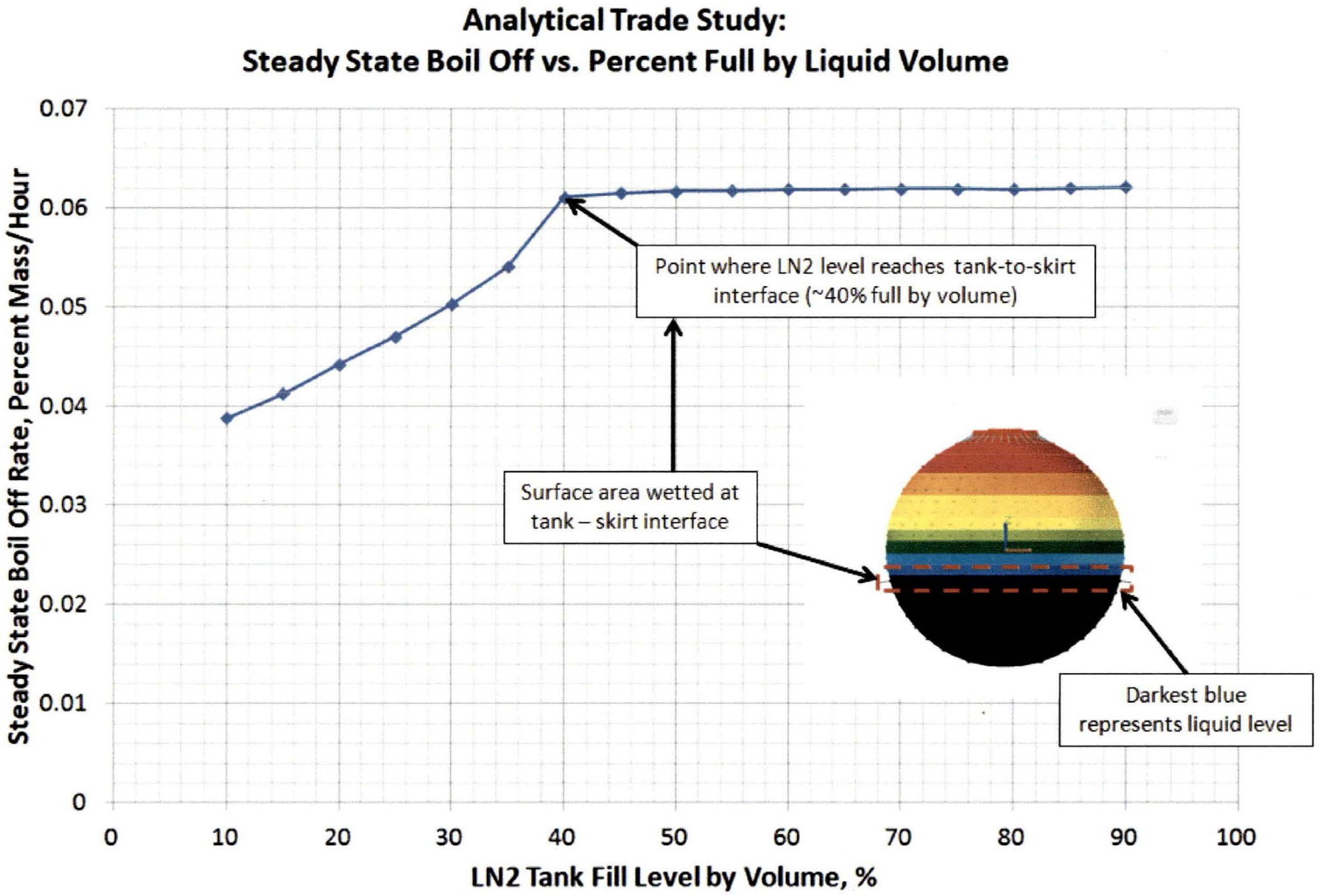

Figure 19: Steady State Boil Off vs. Percent Full by Liquid Nitrogen Volume

CRYOTE GTA Skirt Material Properties Parametric Analysis

- True material properties of composites used in skirt hardware were unavailable
- Analysis below shows most likely conclusions on material properties
- Should be noted that all results prior to this used G-10 properties (well known properties)
- Temperature dependent data was available for IM7-977-2 and G-10 composites
- Thermocouple location 07 was looked at for this analysis since it sat on the bottom-most skirt ring where most significant material mass was located
- Parametric analysis used the following data sets:

G-10 Props

Temp, °R	Thermal Conductivity, BTU/hr-ft-°R	Temp, °R	Specific Heat, BTU/lbm-°R
0	0.046	36	0.024
90	0.179	360	0.159
180	0.260	540	0.239
270	0.329		
360	0.393		
450	0.451		
540	0.503		

IM7 Props

Temp, °R	Thermal Conductivity, BTU/hr-ft-°R	Temp, °R	Specific Heat, BTU/lbm-°R
8	0.272	36	0.007
126	0.578	360	0.119
216	0.636	560	0.185
360	1.130	660	0.218
540	1.940	760	0.246
648	2.510	860	0.265
810	3.760		

Mix

	(G-10)		**(IM7)**
Temp, °R	Thermal Conductivity, BTU/hr-ft-°R	Temp, °R	Specific Heat, BTU/lbm-°R
0	0.046	36	0.007
90	0.179	360	0.119
180	0.260	560	0.185
270	0.329	660	0.218
360	0.393	760	0.246
450	0.451	860	0.265
540	0.503		

Parametric Analysis Results:

Figure below shows that IM7 heat capacity props dominate initial transient temp responses (to about 20hrs) and G-10 thermal conductivity props dominate steady state temps. **Properties for composite materials used in CRYOTE GTA's skirt are between G-10 and IM7 data sets.**

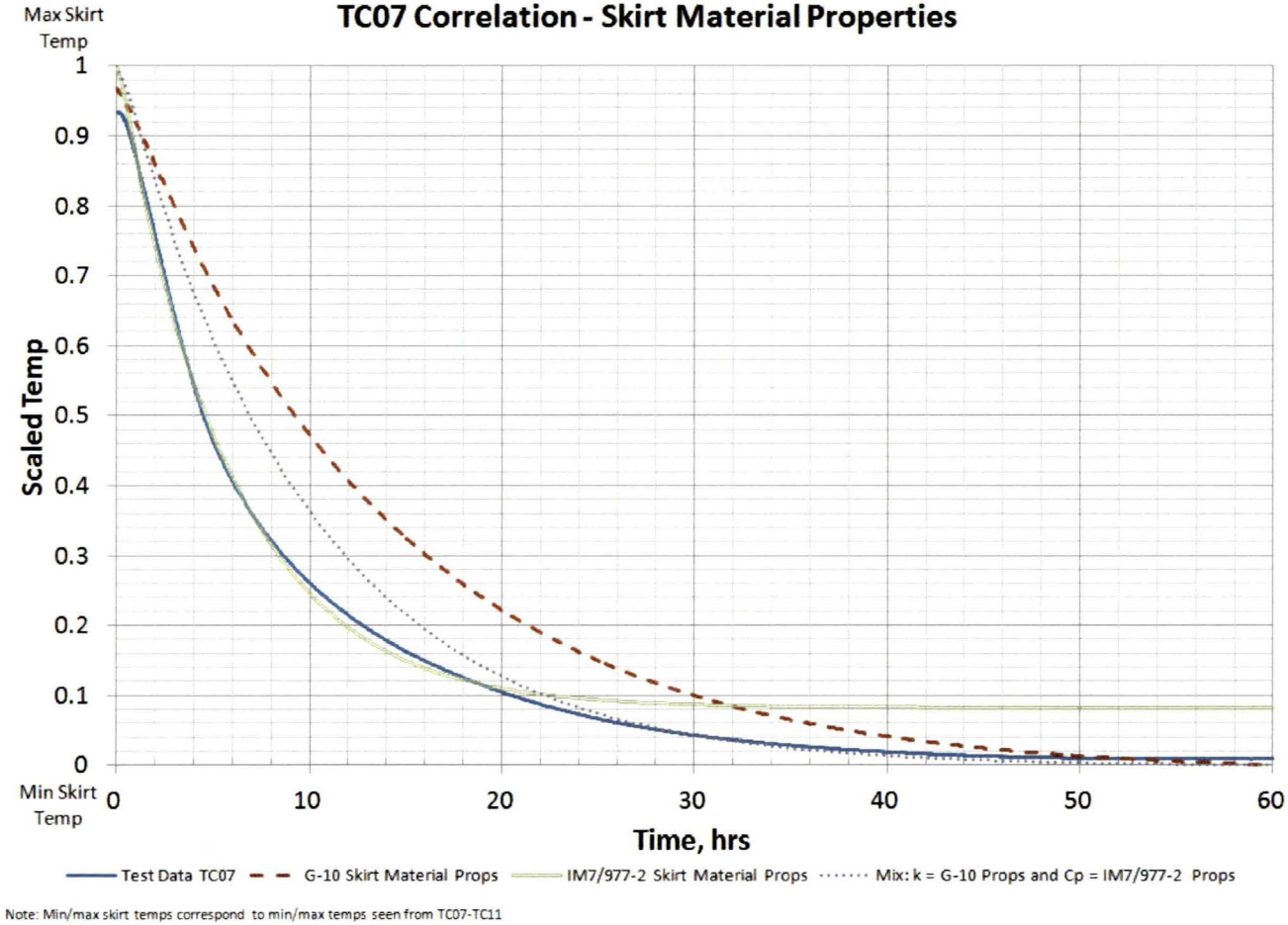

Figure 20: Analytical Trade Study: Skirt Material Properties

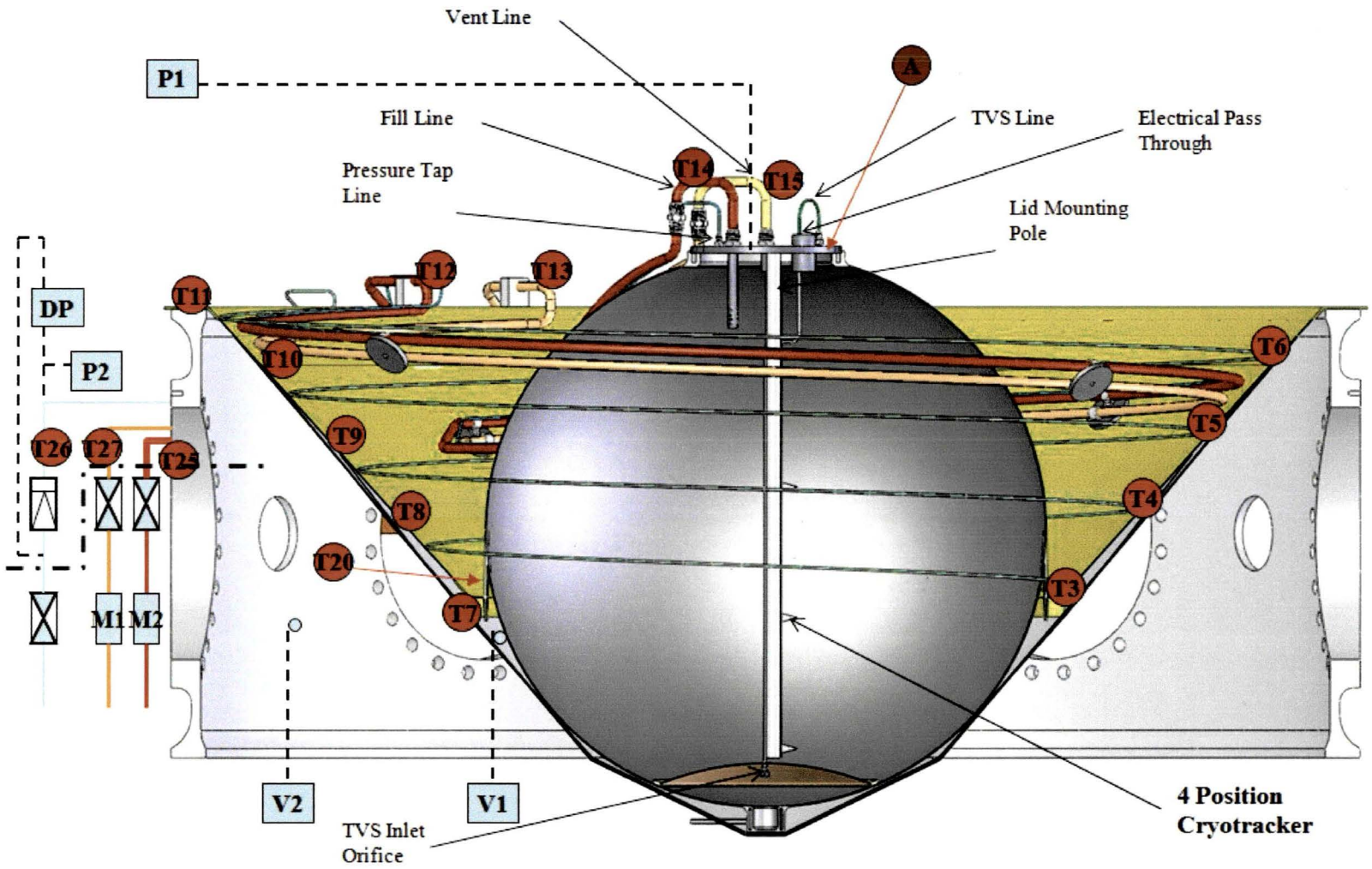

Figure 21: CRYOTE GTA Instrumentation